THE ROYAL SOCIETY

doi 10.1098/rspb.2000.1224

Mechanical performance of aquatic rowing and flying

Jeffrey A. Walker* **and Mark W. Westneat**

Department of Zoology, Field Museum of Natural History, Roosevelt Road at Lake Shore Drive, Chicago, IL 60605, USA

Aquatic flight, performed by rowing or flapping fins, wings or limbs, is a primary locomotor mechanism for many animals. We used a computer simulation to compare the mechanical performance of rowing and flapping appendages across a range of speeds. Flapping appendages proved to be more mechanically efficient than rowing appendages at all swimming speeds, suggesting that animals that frequently engage in locomotor behaviours that require energy conservation should employ a flapping stroke. The lower efficiency of rowing appendages across all speeds begs the question of why rowing occurs at all. One answer lies in the ability of rowing fins to generate more thrust than flapping fins during the power stroke. Large forces are necessary for manoeuvring behaviours such as accelerations, turning and braking, which suggests that rowing should be found in slow-swimming animals that frequently manoeuvre. The predictions of the model are supported by observed patterns of behavioural variation among rowing and flapping vertebrates.

Keywords: swimming performance; unsteady hydrodynamics; energetics; manoeuvrability

1. INTRODUCTION

Many aquatic vertebrates swim through the water by oscillating appendages. The dynamic shape of oscillating appendages varies along a continuum from rowing to flapping (see electronic Appendix A available on The Royal Society Web site). A rowing appendage oscillates anteroposteriorly and has distinct recovery and power strokes (Blake 1979, 1980; Vogel 1994). In contrast to rowing, a flapping appendage oscillates largely dorsoventrally and may or may not present a distinct recovery stroke (Aldridge 1987; Rayner 1993; Walker & Westneat 1997). The presence of both rowing and flapping appendages is found in many different animal groups, including molluscs, crustaceans, insects, fishes, turtles, birds and mammals (Baudinette & Gill 1985; Breder 1926; Davenport *et al*. 1984; Farmer 1970; Fish 1992, 1993, 1996; Plotnick 1985; Satterlie *et al*. 1985; Seibel *et al*. 1998; Vecchione & Young 1997; Williams 1994; Zaret & Kerfoot 1980).

The repeated presence of rowing and flapping in many animal groups needs an explanation: Why do some animals row while others flap? At least three, not mutually exclusive, explanations may be offered. First, rowing is more effective at low Reynolds numbers (Re), while flapping is more effective at high Re, a hypothesis that has not been explored in depth, but it probably occurs as a consequence of the rapidly changing lift to drag ratio on an aerofoil at $Re < 100$ (Thom & Swart 1940). Second, many semi-aquatic animals have to function effectively both on land and in water and an appendage designed for rowing is more suited for walking than an appendage designed for flapping (Fish 1996; Vogel 1994). The third explanation, and the one we explore in this paper, is that rowing is more effective for some behaviours while flapping is more effective for others.

*Author and address for correspondence: Department of Biology, University of Southern Maine, 96 Falmouth Street, Portland, ME 04103, USA (walker@usm.maine.edu).

In the clearest statement of the third explanation, Vogel (1994) found that a rowing plate generates more thrust than a flapping plate at low speeds but the reverse is true at high speeds. For many locomotor behaviours, however, the magnitude of thrust is not as important as the mechanical work required to generate it. This concept is captured by the mechanical efficiency, which is the ratio of useful work to total work. Do Vogel's results imply that rowing is more efficient at low speeds while flapping is more efficient at high speeds?

In order to explore this question, we used a simulation experiment to measure the affects of dynamic shape on the mechanical performance of an oscillating appendage. A quasi-steady blade-element model that accounted for unsteady phenomena such as added mass effects (Daniel 1984), dynamic stall (Dickinson & Götz 1993; Ellington *et al*. 1996), and the cumulative Wagner effect (Dickinson 1994; Dickinson & Götz 1996; Dickinson *et al*. 1999) was used to estimate two performance variables for the oscillating appendage: the mean thrust over a full- and half-stroke cycle and the mechanical efficiency of doing work on the fluid. For readers unfamiliar with the hydromechanics of rowing and flapping, we suggest Vogel (1994) as an introduction and Daniel (1984) and Dickinson (1996) for more details on the unsteady phenomena.

2. METHODS

(a) *Static and dynamic shape*

Each appendage was modelled as a rectangular plate that twisted along its length and oscillated with simple harmonic motion at a constant amplitude of 60° (electronic Appendix A), a typical value for fishes that swim with pectoral fins (Blake 1979; Walker & Westneat 1997; Webb 1973). The appendages oscillated around the flapping axis, which had an angle, β, relative to the free stream. β was 90° for the rowing appendage and 0° for the flapping appendage.

Appendages twisted around the pitching axis giving each element an instantaneous pitch, θ, relative to the flapping axis.

Received 10 April 2000 *Accepted* 2 June 2000

The flapping appendage twisted about its leading edge with simple harmonic motion (figure 1 and electronic Appendix A). We used two different kinematic models of the recovery stroke for the rowing appendage. For one, the rowing appendage twisted about its trailing edge to attain a feathered orientation ($\theta \sim -90^\circ$) during the fore (recovery) stroke and a broadside orientation ($\theta = 0^\circ$) during the backward (power) stroke. We allowed the rowing appendage to rotate quickly into its feathered or broadside orientation by confining twisting to the first third of each stroke (figure 1 and electronic Appendix A). For the second model, we allowed the entire span of the appendage to feather ($\theta = -90^\circ$) throughout the recovery stroke.

(b) *Dumb coefficients*

Blade-element models divide a propulsive structure along its span into a series of blade elements and estimate the force balance on an element using force coefficients that are a function of the element's instantaneous geometry relative to the fluid passing over the element. The basic assumptions of a blade-element model are discussed in Blake (1979). Previous blade-element models of paired-appendage aquatic propulsion used force coefficients (Hoerner 1958) that reflect the time-averaged normal force on the appendage orientated in a uniform velocity flow at a constant angle of attack (Blake 1979, 1985; Fish 1984; Gal & Blake 1988; Hui 1988; Morris *et al.* 1985). The force on a hydrofoil is not only a function of its angle of attack but also of its history of motion. Force coefficients are ignorant of this history. In this study, we attempted to partially model historical effects by using empirically derived lift and drag coefficients measured from root-oscillating plates at Re = 192 (Dickinson *et al.* 1999) and modifying the coefficients by the Wagner function.

The experimental Re of 192 is near the lower bound of the range of Re in which animals both row and flap, but we do not have equivalent experimental data at higher Re. For flat plates translating in a uniform flow at a constant angle of attack, force coefficients are fairly constant for $1000 < \mathrm{Re} < 100\,000$ (Hoerner 1958). Below Re = 100, lift coefficients rise slightly but drag coefficients rise sharply (Thom & Swart 1940). Substitution of the normal force coefficients on a flat plate in a steady flow for Re > 1000 (Hoerner 1958) results in the same performance patterns as occur with the lower Re data.

The use of coefficients from oscillating plates accounts for dynamic stall, a phenomenon that increases the normal force on plates translating at moderate to high attack angles due to the presence of an attached vortex on the downstream surface of the aerofoil (Kuethe & Chow 1986). The Wagner function accounts for the Wagner effect, a phenomenon that decreases the normal force on impulsively starting plates due to the delay in the generation of circulation (Fung 1993). Dickinson (1994) and Dickinson & Götz (1993) showed that dynamic stall overwhelms the Wagner effect if the preceding stroke was at a low attack angle (as in rowing) while the Wagner effect overwhelms the effects of dynamic stall if the preceding stroke was at an intermediate attack angle (as in flapping).

(c) *The model*

We modelled both circulatory forces resulting from velocity differences on opposing sides of the appendage and added mass forces resulting from the acceleration of a mass of fluid. Circulatory thrust ($\mathrm{d}T_\mathrm{c}$), circulatory lift ($\mathrm{d}L_\mathrm{c}$), added mass thrust ($\mathrm{d}T_\mathrm{a}$), and added mass lift ($\mathrm{d}L_\mathrm{a}$) per unit span were computed by (see Fung (1993) and DeLaurier (1993) for similar models)

$$\mathrm{d}T_\mathrm{c} = (-\mathrm{d}F_\mathrm{n}\sin\theta + \mathrm{d}F_\mathrm{x}\cos\theta)\cos\beta - (\mathrm{d}F_\mathrm{n}\cos\theta + \mathrm{d}F_\mathrm{x}\sin\theta)\sin\beta\sin\gamma, \quad (1)$$

$$\mathrm{d}L_\mathrm{c} = (\mathrm{d}F_\mathrm{n}\cos\theta + dF_\mathrm{x}\sin\theta)\cos\beta\sin\gamma + (-\mathrm{d}F_\mathrm{n}\sin\theta + \mathrm{d}F_\mathrm{x}\cos\theta)\sin\beta, \quad (2)$$

$$\mathrm{d}T_\mathrm{a} = \mathrm{d}F_\mathrm{a}\sin\theta\cos\beta + \mathrm{d}F_\mathrm{a}\cos\theta\sin\beta\sin\gamma, \quad (3)$$

$$\mathrm{d}L_\mathrm{c} = -\mathrm{d}F_\mathrm{a}\cos\theta\cos\beta\sin\gamma + \mathrm{d}F_\mathrm{a}\sin\theta\sin\beta, \quad (4)$$

where γ is the positional angle of the appendage with 0° up or back against the body. $\mathrm{d}F_\mathrm{a}$, the added mass force per unit span, was estimated as $\mathrm{d}F_\mathrm{a} = \frac{1}{4}\rho\pi c^2 v'_\mathrm{n}$, where c is chord length and v'_n is the first derivative of the normal velocity component of the chord relative to the water,

$$v_\mathrm{n} = h'\cos\theta + U_\mathrm{n}\sin(\theta + \beta) \pm \tfrac{1}{2}c\theta', \quad (5)$$

where U_n is the flow normal to the span and is found by

$$U_\mathrm{n} = U(1 - |\cos\gamma|\sin\beta). \quad (6)$$

The $\pm$ in equation (5) is positive for the flapping fin, which rotates about the leading edge, and negative for the rowing fin, which rotates about the trailing edge. h' is the tangential velocity of a fin element due to fin oscillation. The normal force per unit span was estimated by

$$\mathrm{d}F_\mathrm{n} = -\mathrm{d}T^*\sin\alpha + \mathrm{d}L^*\cos\alpha, \quad (7)$$

where $\mathrm{d}L^*$ and $\mathrm{d}T^*$ are the components of the circulatory force normal to and parallel with the local stream. α, the hydrodynamic angle of attack, was found by $\alpha = \pm\tan^{-1}(v_\mathrm{n}/v_\mathrm{x})$ where the $\pm$ takes the sign of v_x, the chordwise velocity of the section relative to the fluid

$$v_\mathrm{x} = -h'\sin\theta + U_\mathrm{n}\sin(\theta + \beta). \quad (8)$$

$\mathrm{d}L^*$ and $\mathrm{d}T^*$ were estimated by $\mathrm{d}L^* = \frac{1}{2}\rho c({v_\mathrm{x}}^2 + {v_\mathrm{n}}^2)\phi C_\mathrm{L}$ and $\mathrm{d}T^* = \frac{1}{2}\rho c(v_\mathrm{x}^2 + v_\mathrm{n}^2)\phi C_\mathrm{D}$. The lift and drag coefficients are from Dickinson *et al.* (1999). ϕ, an approximation of the Wagner function, was found by $\phi = 1 - 2/(4 + \tau)$ (Fung 1993), where τ is the number of semi-chords travelled during the stroke. For the rowing strokes, or the flapping strokes in which the Wagner effect was ignored, ϕ was set to unity (see above). The chordwise force per unit span was estimated by $\mathrm{d}F_\mathrm{x} = \frac{1}{2}\rho c v_\mathrm{x}^2 C_\mathrm{sf}$, where C_sf is the coefficient of skin friction drag on the element, $C_\mathrm{sf} = 1.33/\sqrt{\mathrm{Re}}$ (Hoerner 1958). The input power per unit span, due to both circulatory and added mass forces, was estimated by $\mathrm{d}P = \mathrm{d}P_\mathrm{c} + \mathrm{d}P_\mathrm{a}$ where

$$\mathrm{d}P_\mathrm{c} = \mathrm{d}F_\mathrm{n}(h'\cos\theta \pm \tfrac{1}{2}c\theta') + \mathrm{d}F_\mathrm{x}h'\sin\theta, \quad (9)$$

$$\mathrm{d}P_\mathrm{a} = -\mathrm{d}F_\mathrm{a}(h'\cos\theta \pm \tfrac{1}{2}c\theta'). \quad (10)$$

Again, the $\pm$ is positive for the flapping fin and negative for the rowing fin. Thrust, lift and input power were summed across all elements and time increments, multiplied by two to reflect both appendages, and divided by the number of time increments to give mean values. We assumed the appendage worked to accelerate the added mass of water and therefore always used the absolute value of $\mathrm{d}P_\mathrm{a}$.

(d) *The simulation*

We ran the rowing and flapping models for a range of oscillation frequencies and forward speeds in order to describe the mechanical efficiency, η, as a function of reduced frequency, k. η was found by

$$\eta = T_\mathrm{avg}U/P_\mathrm{avg}, \quad (11)$$

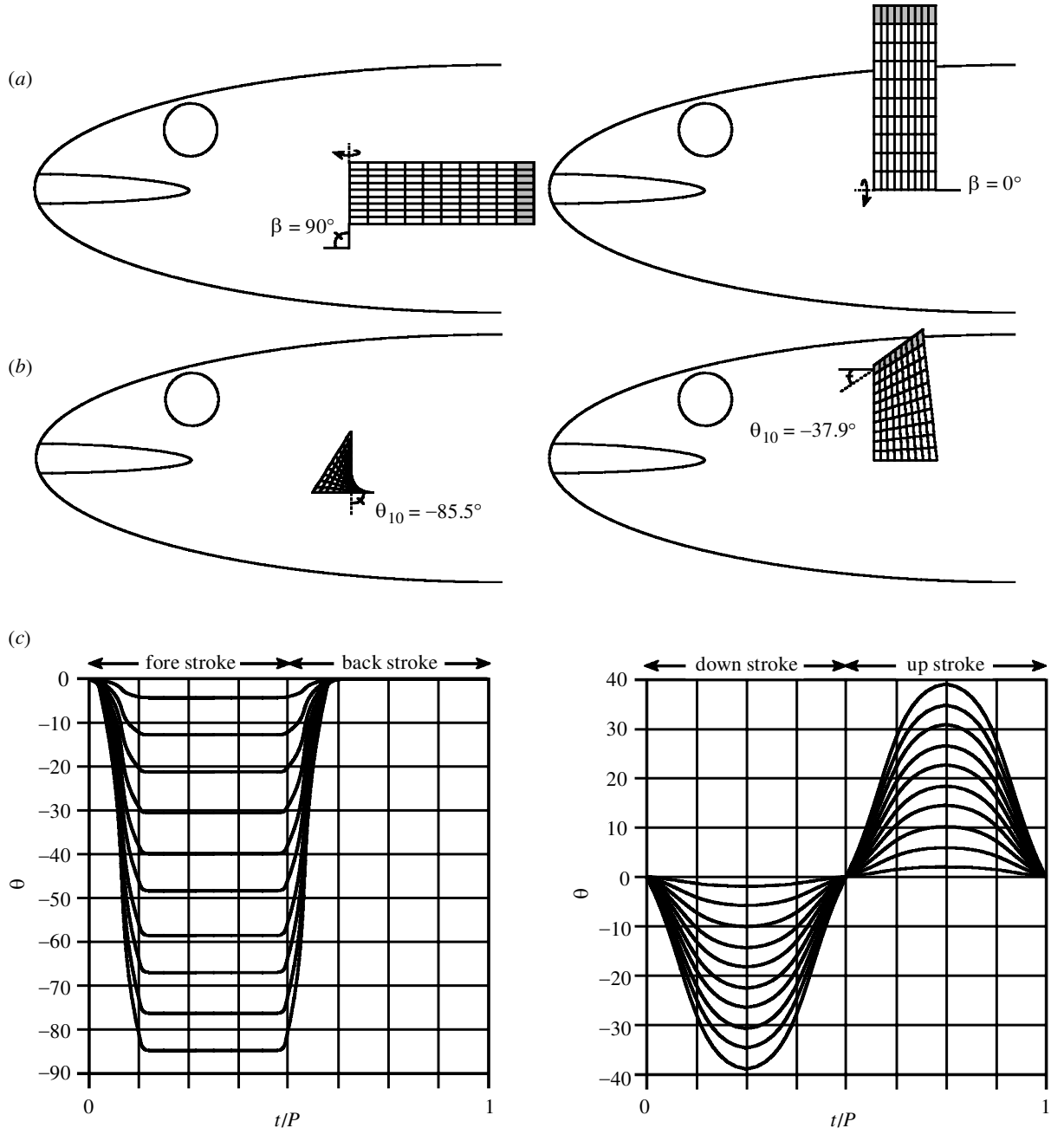

Figure 1. Dynamic shape of oscillating appendage. (*a*) β was 90° for the rowing appendage and 0° for the flapping appendage. Oscillation started from a position that was either back (rowing) or straight up (flapping) with no twist. The most distal element is shaded. (*b*) Appendages dynamically twisted around the pitching axis giving each element an instantaneous pitch, θ, which is shown for the most distal element at its maximum negative pitch. (*c*) θ, for the ten blade elements throughout the stroke cycle. The abscissa is time standardized by the stroke period. See the electronic Appendix A for animations of the rowing and flapping appendage for the data illustrated in (*c*).

where T_{avg} and P_{avg} are the mean thrust and mean input power over the full cycle and U is the forward speed of the animal. The reduced frequency, $k = \omega C/2U$, where ω is circular frequency ($2\pi f$) and C is the mean chord, is a measure of the unsteadiness of the flow velocity over the appendage. For these simulations, we used an appendage with a 3 cm semi-span (appendage length) and 1 cm chord, which is about the size of a pectoral fin of an adult bird wrasse, *Gomphosus varius* (Walker & Westneat 1997).

To measure η as a function of forward speed, we iterated the model, incrementally increasing the stroke frequency by 0.001 Hz, until a frequency was reached in which T balanced the drag on a simulated body. For this drag, we used the theoretical drag on a body of revolution with a length of 15 cm and a radius of $\sqrt{8}$ cm (Hoerner 1958). Again, these dimensions are about the size of the body of a bird wrasse (Walker & Westneat 1997).

At each speed and stroke frequency, η of the flapping fin was computed for all twist amplitudes that resulted in a maximum pitch between $\pm 1°$ and $\pm 90°$ (in increments of 1°) for the distal element of the appendage. For the rowing fin, all twist amplitudes that resulted in a maximum recovery stroke pitch between $-90°$ and $-150°$ (in increments of 1°) for the distal element were computed. We held the pitch of the distal element

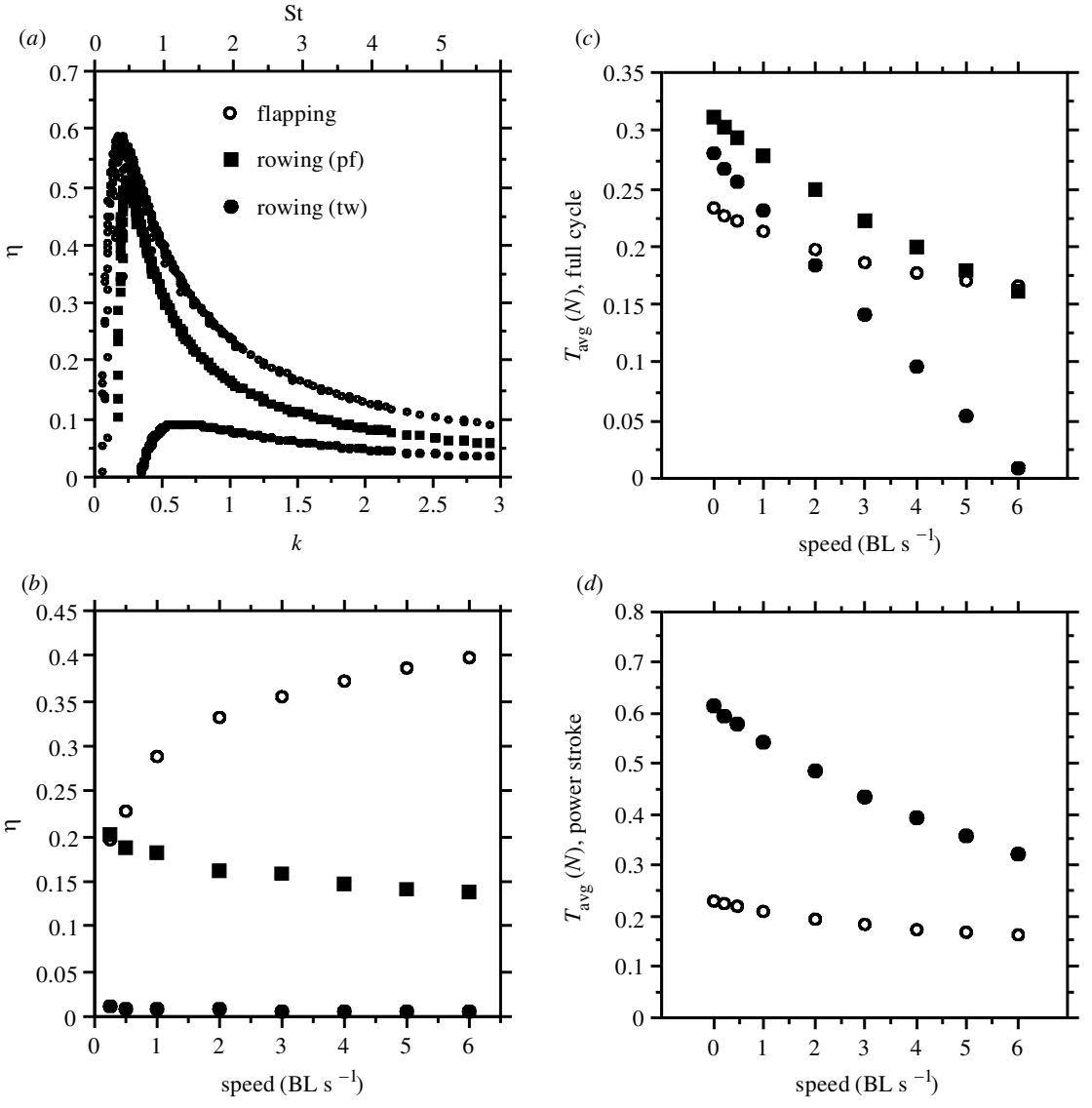

Figure 2. Mechanical efficiency, η, and mean thrust, T, of paired rowing or flapping appendages. (*a*) η as a function of reduced frequency, k, and St. (*b*) η as a function of speed. (*c*, *d*). Mean thrust over the (*c*) full cycle and (*d*) power stroke (up stroke for flapping appendage and back stroke for rowing appendage). Mean thrust was computed for simulated appendages that oscillated at a frequency of 10 Hz. The dynamic twist that resulted in the maximum thrust is compared.

following the supination at the beginning of the power stroke at a constant 0° (figure 1). For both rowing and pitching fins, the magnitude of the pitch amplitude that maximized either η or average thrust was chosen for the comparisons.

3. RESULTS

The geometry of the recovery stroke greatly influenced the mechanical performance of a rowing appendage (figure 2). Peak η was 0.51 at $k = 0.24$ for the feathered rowing appendage but only 0.09 at $k = 0.64$ for the twisted rowing appendage. The flapping appendage, with a peak $\eta = 0.59$ at $k = 0.18$, oscillated with higher η than the rowing appendage at all k (figure 2*a*).

For the body simulated here, the flapping appendage generated the necessary force to balance body drag with higher η at all swimming speeds (figure 2*b*). For the flapping fin, η increased steeply with swimming speed, from 0.2 at $0.25\,\mathrm{BL\,s^{-1}}$ ($k = 0.17$) to 0.4 at $6\,\mathrm{BL\,s^{-1}}$ ($k = 0.12$). Again, performance of the rowing appendage depended on the geometry of the recovery stroke. η decreased from 0.20 at $0.25\,\mathrm{BL\,s^{-1}}$ ($k = 0.18$) to 0.14 at $6\,\mathrm{BL\,s^{-1}}$ ($k = 0.17$) for the feathered rowing appendage and from 0.011 at $0.25\,\mathrm{BL\,s^{-1}}$ ($k = 0.36$) to 0.006 at $6\,\mathrm{BL\,s^{-1}}$ ($k = 0.34$) for the twisted rowing appendage.

Over the entire stroke cycle, the twisted rowing appendage generated more thrust than the flapping appendage only at slow speeds while the feathered rowing appendage generated more thrust than the flapping appendage over much of the speed range (figure 2*c*). Over the power stroke, mean thrust of either rowing appendage greatly exceeded that for the flapping appendage at all speeds (figure 2*d*).

4. DISCUSSION

The goal of this simulation experiment was to measure the effect of appendage motion (rowing or flapping) on the mechanical performance of an oscillating appendage by holding constant the effects of other variables that

potentially influence performance, such as fin shape, amplitude, and phase differences between pitching and oscillation. We did model two different recovery strokes for the rowing appendage: a spanwise twisting appendage and a perfectly feathered appendage. Animals can only approximate a perfectly feathered appendage along the entire span throughout the recovery stroke. For example, the sequential peeling off of the fin rays from the same dorsoventral position on the body allows fishes to feather most of the fin, and jointed limbs allow nearly optimal feathering of the distal limb in secondarily aquatic tetrapods. Our two rowing models should set upper and lower bounds on the mechanical performance of real limbs.

The experiment has three important results. First, these are the first direct comparisons of η for rowing and flapping appendages oscillating in the same hydrodynamic environment. We compare our model with experimental data and find good agreement. Second, flapping appendages are more mechanically efficient than rowing appendages at all speeds. We discuss the behavioural consequences of this energetic difference. Finally, at slow speeds, flapping appendages are more efficient but rowing appendages generate more thrust. Large thrust, in turn, facilitates manoeuvrability. We suggest that the performance trade-off at slow speeds explains the presence of rowing in some aquatic vertebrates, especially fishes.

(a) *Evaluation of the model*

Results from the model can be usefully compared with the efficiencies measured from motor-driven rowing and flapping appendages. A motor-driven rowing fin with a fan-shaped planform had a maximum $\eta = 0.1$–0.15 at $k = 2$ (Kato 1999) compared with $\eta = 0.09$ and 0.04 for our feathered and twisted rowing appendages at $k = 2$ (figure 2*b*). A motor-driven flapping wing that passively twisted along its span had an η in the range 0.1–0.5 (Archer *et al*. 1979). Importantly, their empirical data fit a theoretical model, which they developed, whose results can be more easily compared with the data presented here. For the Archer *et al*. model, peak $\eta = 0.65$ occurred at $k = 0.21$ and with a twist amplitude of 40° at the distal tip. By comparison, the peak $\eta = 0.59$ of our flapping model occurred at $k = 0.18$ and a twist amplitude of 48°. Given these comparisons, we believe our simple, blade-element model is quite sufficient to evaluate rowing versus flapping performance.

It has been shown that the efficiency of heaving (linear oscillation) and pitching aerofoils is associated with the geometry of the vortex wake (Anderson *et al*. 1998). Optimal wake geometry for maximizing η, the reverse von Karmen vortex street, occurs when the non-dimensional Strouhal number (St), fA/U, where A is the maximum displacement of the oscillating aerofoil (a proxy for the width of the wake), is 0.3–0.4 (Anderson *et al*. 1998). Peak efficiency of our flapping appendage occurred at St = 0.37 (figure 2*a*). The St of aquatic animals swimming with a caudal fin oscillation was in the range 0.25–0.35. The St of the flapping stroke of the bird wrasse ranged from 0.54 at about 1.5 BL s^{-1} to 0.31 at 4 BL s^{-1} (Walker & Westneat 1997).

How do our results compare with estimates of mechanical efficiency of rowing and flapping animals? Using oxygen consumption data, Webb (1974) found $\eta = 0.6$–0.65 for the flapping stroke of the surf-perch, *Cymatogaster aggregata* swimming at $k = 0.25$. For our model flapping appendage, we found a peak $\eta = 0.58$ at $k = 0.25$ (figure 2*b*).

Using a simple blade-element model, Blake (1979, 1980) computed an η of 0.16 for the rowing stroke of the freshwater angelfish, *Pterophyllum emekei*, swimming at 0.5 TL s^{-1} and $k = 2.1$. This is substantially larger than the corresponding value of $\eta = 0.08$ for our model rowing appendage with perfect feathering at the same k. We believe Blake's estimate is inflated due to his substitution of the dead drag of the individual with its pectoral fins extended for $\bar{T}_{avg}$ in equation (11). While swimming at a uniform speed, $\bar{T}_{avg}$ summed over both fins should equal the sum of the body drag with the fins folded against the body and the net skin friction drag on the fins, which should be small relative to the drag on the body. If we substitute Blake's measure of the dead drag of the fish with its fins folded against its body into equation (11), we compute a revised estimate as $\eta = 0.037$. This value is close to the value of 0.047 for the twisted, rowing appendage at $k = 2.1$.

(b) *Consequences of an efficient flapping stroke*

Is performance variation among real animals consistent with the simulation results? The high efficiency of flapping appendages suggests that flapping animals might have higher critical swimming speeds and lower costs of transport (COT), while cruising at largely uniform speeds, relative to rowing animals. In a direct comparison between four species of wrasse (Labridae), the two flapping species had significantly higher critical swimming speeds than the two rowing species (Westneat & Walker 1997).

Comparisons of the COT among rowing and flapping vertebrates (Fish 1992, 1993; Fish *et al*. 1997; Videler & Nolet 1990) show that sea turtles and sea lions, which flap their appendages, have lower COTs than ducks, mink, and muskrat, which paddle at the surface. Contrary to simulation results, however, flapping penguins have COTs similar to those of the surface-paddling animals while the rowing platypus has a COT expected of sea turtles and sea lions (Fish *et al*. 1997). Because surface swimming is more energetically expensive than submerged swimming (Baudinette & Gill 1985; Videler & Nolet 1990), the interacting effects of swimming location and swimming gait confound these comparisons.

The higher η of the flapping appendage also suggests that animals that need to cruise at some constant speed for prolonged periods should employ a flapping gait. Sea turtles, which can both row their hindlimbs and flap their forelimbs, migrate hundreds to thousands of kilometres between foraging and nesting areas (Wyneken 1997). Available field observations indicate that adult green turtles and loggerheads employ a flapping geometry exclusively for these migrations (Wyneken 1997). Of the many semi-aquatic and aquatic mammals that propel themselves with oscillating appendages, only species that flap their appendages, the fur seals and sea lions (Otariidae) (Feldkamp 1987*a*,*b*), make aquatic migrations (Riedman 1990).

The three-spined stickleback, *Gasterosteus aculeatus*, provides an intriguing exception to the hypothesis that

aquatic, paired appendage cruisers should flap instead of row. Anadromous and marine populations make long migrations between spawning and winter feeding sites (Cowen *et al*. 1991). *G. aculeatus* employs pectoral fin oscillation to the exclusion of axial undulation until fatigue velocities are reached (Stahlberg & Peckmann 1987; Taylor & McPhail 1986; Walker 1999; Whoriskey & Wootton 1987). Contrary to the hypothesis that cruising animals should prefer a flapping to a rowing stroke, the stickleback presents a stereotypical rowing geometry at all subcritical swimming speeds (Walker 1999). This observation may reflect a constraint on the design of the juvenile stickleback pectoral fin. The pectoral fin of a juvenile stickleback swimming at one to two body lengths per second would operate at a Re of *ca.* 10–50, a range that may preclude effective use of a circulatory lift-based mechanism of propulsion (Thom & Swart 1940).

(c) *Performance trade-offs: efficiency versus manoeuvrability*

It has been suggested that rowing propulsion is more efficient than axial propulsion at slow speeds and should be the preferred gait for slow-speed swimming and manoeuvring (Blake 1979, 1980; Webb & Blake 1985). But why not flap at low speeds, given that flapping is less costly than rowing at all speeds? At low speeds, rowing does generate more thrust than flapping (figure 2; see also Vogel 1994). For cruising at low speeds, however, low thrust production should not handicap a flapping appendage since it can simply oscillate at a higher frequency and still be more energetically efficient than the rowing appendage.

But slowly swimming animals do not generally swim at uniform speeds. Instead, slowly swimming animals frequently accelerate forwards, turn and brake. These behaviours are facilitated by large thrust or drag generated by the paired appendages. This suggests that limb design for animals that prefer to swim at slow speeds are constrained by a performance trade-off. To maximize energy efficiency, flapping appendages are most effective. To maximize manoeuvrability, rowing appendages are most effective. Manoeuvring performance should be related more to the force generated during the power stroke and not averaged over both strokes. We found the advantage of the rowing fin for generating thrust at slow speeds increased sharply after considering only the power stroke (figure 2*d*).

These results suggest that rowing should be associated with slow-speed swimming and especially manoeuvring whereas flapping should be associated with the ability to achieve high swimming speeds (Vogel 1994). Indeed, many fishes row with their fins for slow-speed swimming and manoeuvring but switch to axial undulation to achieve higher speeds (Webb 1993, 1994). The highest pectoral-fin-powered speeds are achieved in species of Acanthuridae (surgeon fish), Pomacentridae (damselfish), Scaridae (parrot fish), Embiotocidae (surf-perches) and Labridae (wrasses) that flap the pectoral fins (Walker & Westneat 1997; Webb 1993, 1994; Westneat & Walker 1997).

Data from turtles also support the predictions of the model. Laboratory comparisons of marine and freshwater turtles indicate that the green sea turtle, *Chelonia mydas*, reached a maximum speed of *ca.* 13 BL s^{-1} using flapping foreflippers (Davenport & Pearson 1994). By contrast, the freshwater turtle *Mauremys caspica* attained a top speed of about 2.2 BL s^{-1} using simultaneous fore- and hindlimb rowing (Davenport & Pearson 1994).

Additionally, available data show that nearly all sea turtles, at least as post-hatchlings and juveniles, switch gaits to achieve faster speeds. During their pelagic phase, sea turtles tend to swim slowly at the surface using hindlimb rowing strokes but switch to a forelimb flapping gait for escape behaviours (Davenport *et al*. 1997; Davenport & Pearson 1994; Wyneken 1997). By contrast, post-hatchling sea turtles predominantly employ a flapping stroke at the onset of relatively high-speed, offshore migrations (Wyneken 1997).

(d) *Combining comparative and experimental data*

This study demonstrates the value of combining comparative studies with experimental models that address the causal relationship between phenotype and performance. Performance differences between rowers and flappers may reflect variation in the shape of the appendage, morphology of the shoulder and joints, motor control of the limb muscles, contractile properties of muscle tissue, shape and design of the body, and performance of the oxygen transport system. Despite the wide range of variables influencing locomotor ability, the simulations of aquatic flight in this study suggest specific functional roles for flapping and rowing appendages and explain patterns of phenotypic diversity that have repeatedly evolved in many animal groups.

This work was stimulated by Steven Vogel's *Life in moving fluids*. Discussions with Michael Dickinson, Brad Wright and Rick Blob helped to clarify our ideas. This work was supported by Office of Naval Research Grant N00014-99-1-0184, National Science Foundation grant DEB-9815614, a National Science Foundation Postdoctoral Research Fellowship in the Biosciences Related to the Environment and a research fellowship from Berkeley Research Associates.

REFERENCES

Aldridge, H. D. J. N. 1987 Body accelerations during the wingbeat in six bat species: the function of the upstroke in thrust generation. *J. Exp. Biol.* **130**, 275–293.

Anderson, J. M., Streitien, K., Barrett, D. S. & Triantafyllou, M. S. 1998 Oscillating foils of high propulsive efficiency. *J. Fluid Mech.* **360**, 41–72.

Archer, R. D., Sapuppo, J. & Betteridge, D. S. 1979 Propulsion characteristics of flapping wings. *Aeronaut. J.* **83**, 355–371.

Baudinette, R. V. & Gill, P. 1985 The energetics of 'flying' and 'paddling' in water: locomotion in penguins and ducks. *J. Comp. Physiol.* B **155**, 373–380.

Blake, R. W. 1979 The mechanics of labriform locomotion. I. Labriform locomotion in the angelfish (*Pterophyllum eimekei*): an analysis of the power stroke. *J. Exp. Biol.* **82**, 255–271.

Blake, R. W. 1980 The mechanics of labriform locomotion. II. An analysis of the recovery stroke and the overall fin-beat cycle propulsive efficiency in the angelfish. *J. Exp. Biol.* **85**, 337–342.

Blake, R. W. 1985 Hydrodynamics of swimming in the water boatman, *Cenocorixa bifida*. *Can. J. Zool.* **64**, 1606–1613.

Breder Jr, C. M. 1926 The locomotion of fishes. *Zoologica* **4**, 159–291.

Cowen, R. K., Chiarella, L. A., Gomez, C. J. & Bell, M. A. 1991 Offshore distribution, size, age, and lateral plate variation of late larval/early juvenile sticklebacks (*Gasterosteus*)

off the Atlantic coast of New Jersey and New York. *Can. J. Fish. Aquat. Sci.* **48**, 1679–1684.
Daniel, T. L. 1984 Unsteady aspects of aquatic locomotion. *Am. Zool.* **24**, 121–134.
Davenport, J. & Pearson, G. A. 1994 Observations on the swimming of the Pacific ridley, *Lepidochelys olivacea* (Eschscholtz, 1829): comparisons with other sea turtles. *Herpetol. J.* **4**, 60–63.
Davenport, J., Munks, S. A. & Oxford, P. J. 1984 A comparison of the swimming of marine and freshwater turtles. *Proc. R. Soc. Lond.* B **220**, 447–475.
Davenport, J., de Verteuil, N. & Magill, S. 1997 The effects of current velocity and temperature upon swimming in juvenile green turtles *Chelonia mydas* L. *Herpetol. J.* **7**, 143–147.
DeLaurier, J. D. 1993 An aerodynamic model for flapping-wing flight. *Aeronaut. J.* **97**, 125–130.
Dickinson, M. H. 1994 The effects of wing rotation on unsteady aerodynamic performance at low Reynolds numbers. *J. Exp. Biol.* **192**, 179–206.
Dickinson, M. H. 1996 Unsteady mechanisms of force generation in aquatic and aerial locomotion. *Am. Zool.* **36**, 537–554.
Dickinson, M. H. & Götz, K. G. 1993 Unsteady aerodynamic performance of model wings at low Reynolds numbers. *J. Exp. Biol.* **174**, 45–64.
Dickinson, M. H. & Götz, K. G. 1996 The wake dynamics and flight forces of the fruit fly *Drosophila melanogaster*. *J. Exp. Biol.* **199**, 2085–2104.
Dickinson, M. H., Lehmann, F.-O. & Sane, S. P. 1999 Wing rotation and the aerodynamic basis of insect flight. *Science* **284**, 1954–1960.
Ellington, C. P., Van den Berg, C. & Willmott, A. P. 1996 Leading-edge vortices in insect flight. *Nature* **384**, 626–630.
Farmer, W. M. 1970 Swimming gastropods (Opistobranchia and Prosobranchia). *Veliger* **13**, 73–89.
Feldkamp, S. D. 1987*a* Foreflipper propulsion in the California sea lion, *Zalophus californianus*. *J. Zool.* **212**, 43–57.
Feldkamp, S. D. 1987*b* Swimming in the California sea lion: morphometrics, drag, and energetics. *J. Exp. Biol.* **131**, 117–135.
Fish, F. E. 1984 Mechanics, power output and efficiency of the swimming muskrat (*Ondatra zibethicus*). *J. Exp. Biol.* **110**, 183–201.
Fish, F. E. 1992 Aquatic locomotion. In *Mammalian energetics: interdisciplinary views of metabolism and reproduction* (ed. T. E. Tomasi & T. H. Horton), pp. 34–63. Cornell University Press.
Fish, F. E. 1993 Influence of hydrodynamic design and propulsive mode on mammalian swimming energetics. *Aust. J. Zool.* **42**, 79–101.
Fish, F. E. 1996 Transitions from drag-based to lift-based propulsion in mammalian swimming. *Am. Zool.* **36**, 628–641.
Fish, F. E., Baudinette, R. V., Frappell, P. B. & Sarre, M. P. 1997 Energetics of swimming by the platypus *Ornithorhynchus anatinus*: metabolic effort associated with rowing. *J. Exp. Biol.* **200**, 2647–2652.
Fung, Y. C. 1993 *An introduction to the theory of aeroelasticity*. New York: Dover.
Gal, J. M. & Blake, R. W. 1988 Biomechanics of frog swimming. I. Estimation of the propulsive force generated by *Hymenochirus boettgeri*. *J. Exp. Biol.* **138**, 399–411.
Hoerner, S. F. 1958 *Fluid-dynamic drag*. Midland Park, NJ: Published by the author.
Hui, C. A. 1988 Penguin swimming. I. Hydrodynamics. *Physiol. Zool.* **61**, 333–342.
Kato, N. 1999 Hydrodynamic characteristics of mechanical pectoral fin. *J. Fluid Eng.* **121**, 605–613.
Kuethe, A. M. & Chow, C.-Y. 1986 *Foundations of aerodynamics*. New York: Wiley.
Morris, M. J., Gust, G. & Torres, J. J. 1985 Propulsion efficiency and cost of transport for copepods: a hydromechanical model of crustacean swimming. *Mar. Biol.* **86**, 283–295.
Plotnick, R. E. 1985 Lift based mechanisms for swimming in eurypterids and portunid crabs. *Trans. R. Soc. Edinb.* **76**, 325–337.
Rayner, J. M. V. 1993 On aerodynamics and energetics of vertebrate flapping flight. *Contemp. Math.* **141**, 351–400.
Riedman, M. 1990 *The pinnipeds*. Berkeley, CA: University of California Press.
Satterlie, R. A., LaBarbera, M. & Spencer, A. N. 1985 Swimming in the pteropod mollusc, *Clione limacina*. *J. Exp. Biol.* **116**, 189–204.
Seibel, B. A., Thuesen, E. V. & Childress, J. J. 1998 Flight of the vampire: ontogenetic gait-transition in *Vampyroteuthis infernalis* (Cephalopoda: Vampyromorpha). *J. Exp. Biol.* **201**, 2413–2424.
Stahlberg, S. & Peckmann, P. 1987 The critical swimming speed of small teleost fish species in a flume. *Arch. Hydrobiol.* **110**, 179–193.
Taylor, E. B. & McPhail, J. D. 1986 Prolonged and burst swimming in anadromous and freshwater threespine stickleback, *Gasterosteus aculeatus*. *Can. J. Zool.* **64**, 416–420.
Thom, A. & Swart, P. 1940 Forces on an airfoil at very low speeds. *J. R. Aero. Soc.* **44**, 761–770.
Vecchione, M. & Young, R. E. 1997 Aspects of the functional morphology of cirrate octopods: locomotion and feeding. *Vie Milieu* **47**, 101–110.
Videler, J. J. & Nolet, B. A. 1990 Costs of swimming measured at optimum speed: scale effects, differences between swimming styles, taxonomic groups and submerged and surface swimming. *Comp. Biochem. Physiol.* A **97**, 91–99.
Vogel, S. 1994 *Life in moving fluids*, 2nd edn. Princeton University Press.
Walker, J. A. 1999 Pectoral fin rowing is a drag. *Am. Zool.* **38**, 18A.
Walker, J. A. & Westneat, M. W. 1997 Labriform propulsion in fishes: kinematics of flapping aquatic flight in the bird wrasse *Gomphosus varius* (Labridae). *J. Exp. Biol.* **200**, 1549–1569.
Webb, P. W. 1973 Kinematics of pectoral fin propulsion in *Cymatogaster aggregata*. *J. Exp. Biol.* **59**, 697–710.
Webb, P. W. 1974 Efficiency of pectoral fin propulsion of *Cymatogaster aggregata*. In *Swimming and flying in nature*, vol. 2 (ed. T. Y. Wu, C. J. Brokaw & C. Brennen), pp. 573–584. New York: Plenum.
Webb, P. W. 1993 Swimming. In *The physiology of fishes* (ed. D. H. Evans), pp. 47–73. Boca Raton, FL: CRC Press.
Webb, P. W. 1994 Exercise performance of fish. In *comparative vertebrate exercise physiology: phyletic adaptations* (ed. J. H. Jones), pp. 1–49. San Diego, CA: Academic Press.
Webb, P. W. & Blake, R. W. 1985 Swimming. In *Functional vertebrate morphology* (ed. M. Hildebrand, D. M. Bramble, K. F. Liem & D. B. Wake), pp. 110–128. Harvard University Press.
Westneat, M. W. & Walker, J. A. 1997 Applied aspects of mechanical design, behavior, and performance of pectoral fin swimming in fishes. In *Proceedings of unmanned, untethered, submersible technology, 1997*. Durham, NH: Autonomous Underwater Systems Institute.
Whoriskey, F. G. & Wootton, R. J. 1987 The swimming endurance of threespine sticklebacks, *Gasterosteus aculeatus* L., from the Afon Rheidol, Wales. *J. Fish Biol.* **30**, 335–339.
Williams, T. A. 1994 A model of rowing propulsion and the ontogeny of locomotion in *Artemia* larvae. *Biol. Bull.* **187**, 164–173.
Wyneken, J. 1997 Sea turtle locomotion: mechanics, behavior, and energetics. In *The biology of sea turtles* (ed. P. L. Lutz & J. A. Musick), pp. 165–198. Boca Raton, FL: CRC Press.
Zaret, R. E. & Kerfoot, W. C. 1980 The shape and swimming technique of *Bosmina longirostris*. *Limnol. Oceanogr.* **25**, 126–133.

As this paper exceeds the maximum length normally permitted, the authors have agreed to contribute to production costs.

An electronic appendix to this paper can be found at http://www.pubs.royalsoc.ac.uk.